https://doi.org/10.15407/ufm.25.02.364

N.A. GURBANOV
Azerbaijan State Oil and Industry University,
Azadlig, 20,
AZ-1010 Baku, Azerbaijan
nurlan.gurbanov@asoiu.edu.az

EXPERIMENTAL AND FINITE ELEMENT METHODS IN DETERMINING THE FLEXURAL PROPERTIES OF FIBRE METAL LAMINATE COMPOSITES

The study consisting of two stages is carried out to better interpret the damage processes occurring in fibre metal laminate (FML) composite samples. At the first stage, a three-dimensional geometric-data-based model of FML composites is created using the finite element method and used to predict the flexural strength properties according to the ASTM D3039M standard. At the second stage, 7075-T6 Al matrix FML composite samples with 0.0% epoxy, 0.2% graphene, 0.2% SiO_2, and 0.2% clay nanoparticles' addition are prepared in the laboratory environment in line with the numerical model, and their flexural strength properties are examined. As a result of the experiments, it is observed that the addition of 0.2% SiO_2 nanoparticles improves the flexural strength properties of 7075-T6 Al matrix FML composite samples by 50.2% in comparison with such properties of composites prepared with epoxy resin. This value is the highest bending-strength value among sample groups with the same ratio. As a result of the studies, it is observed that there is a 5% difference between the flexural-test results for the FML composite samples made according to the ASTM D3039M standard and the simulation results made within the ANSYS program.

Keywords: FML composite, flexural strength, nanoparticle, finite element method.

Citation: N.A. Gurbanov, Experimental and Finite Element Methods in Determining the Flexural Properties of Fibre Metal Laminate Composites, *Progress in Physics of Metals*, **25**, No. 2: 364–385 (2024)

1. Introduction

1.1. Development, Advantages, and Properties of FML Composites

Rapidly developing technologies in engineering applications and everyday life always require new materials to meet the growing needs of the industry. Especially in the industry, materials with high strength, long life, cheap, light, environmentally friendly and high mechanical properties are required [1, 2]. Composites have recently come to the fore as the main group of materials that can meet these requirements [3]. Composites are a group of materials resulting from the combination of two or more materials with different properties at the macro level using different physical methods for a specific purpose [1–4].

After the Second World War, composite materials were increasingly used, especially in the aviation industry, thanks to their high corrosion and fatigue resistance and high strength [2, 5]. However, the low-impact behaviour of composite materials has led to the development of hybrid FML composites with high-impact behaviour [3, 6]. Hybrid FML composites are a type of material that combines the advantages of both metal and fibre-reinforced polymer composites [5–7]. It consists of alternating metal and fibre-reinforced polymer layers forming a layered structure with increased mechanical properties (Fig. 1) [8]. Metal layers provide high strength and stiffness, while fibre-reinforced polymer layers increase the fatigue resistance, impact resistance and damage tolerance of the composite. By combining these two materials, the hybrid FML composite can exhibit superior mechanical performance compared to conventional metal or polymer composites alone [9, 10].

In 1980, the development of ARALL (Aramid Reinforced Aluminium Laminates) composites began by the National Aerospace Laboratory and Delft University of Technology, the Netherlands [11]. Later, CARALL (Carbon Reinforced Aluminium Laminates), and GLARE (Glass Reinforced Aluminium Laminates) composites were developed to improve the mechanical properties of FMLs [11, 12]. Apart from these, the use of different materials such as magnesium instead of aluminium in FMLs was also tried, but the desired impact, fatigue and static properties could not be obtained [13, 14].

The fibres in FML composite structures have high fatigue resistance because they restrict the propagation of a crack that may start anywhere in the composite and act as a bridge [15, 16]. At the same time, FML composites are used as structural materials with high strength, thanks to monolithic metal sheets with high load-bearing strength and fibres with high strength and hardness [15, 17]. FML composites have excellent moisture and corrosion resistance, and degradation of FMLs because of environmental conditions is significantly lower compared to metallic structures or composite structures [15].

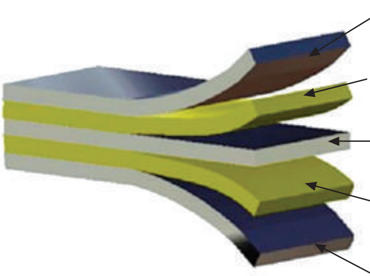

Fig. 1. Hybrid FML composite material [8]

Hybrid FML composite structures are widely used in various aerospace industries due to their superior properties [18]. FML composite structures used in aviation industries must bear different loads such as tension [19], flexural [17], and fatigue [20] throughout their service life.

The use of different amounts of nanoparticles as reinforcement materials in composites to improve the bending properties of hybrid FML structures and increase the adhesive adhesion between sheets has been reported in the literature in different studies [21–24].

In Ref. [25], authors examined the effects of clay nanoparticle additions at different rates on the flexural properties of 2024-T3 Al matrix hybrid FML composites. As a result of the experiments, the positive effects of clay nanoparticles on the bending properties of composite samples were determined.

The effects of 0.0, 0.1, 0.25, and 0.5% GNP additions on the flexural properties of the 2024-T3 Al matrix hybrid FML composite were studied in Ref. [26]. As a result of the experiments, it was determined that the addition of 0.1% GNP significantly improved the flexural strength and modulus of the samples compared to the other composites tested.

Authors of Ref. [27] examined the mechanical properties of GLARE composites prepared following the 2/1 stacking order, reinforced with nanoparticles such as SiO_2, Al_2O_3, aluminium, copper and titanium oxide at 1 wt.%. As a result, they observed that composite samples with SiO_2 nanoparticles added maximum improvements in flexural strength and flexural stiffness, approximately 15% and 36.9%, compared to other GLARE sample groups.

At the same time, the flexural strength of FML composites may be affected by factors such as metal surface treatment [28]. Various processing methods have been proposed in the literature to improve the adhesive bond between the composite layer and the metal surface of FMLs [29]. These methods include mechanical, chemical, electrochemical, coupling agents and dry surface treatments [30, 31].

Newaz [32] examined the impact behaviour of carbon fibre-reinforced Al sheet composites using experimental and finite element analysis. In their study, they determined that polyester resin reinforcement reduced the delamination area caused by crack formation at the interface of aluminium sheets and fibre by 45–50%.

Many experimental and theoretical studies have been carried out. The force–displacement behaviour of two different composite materials was compared experimentally and numerically using the ANSYS finite element method. As a result of these studies, the numerical solution and the experimental solution gave similar results [33].

Finite element models can provide a cost-effective and time-efficient alternative to laboratory testing to understand the damage process of FML composites [34, 35]. With the recent development of technology, the mechanical properties of FML composites are examined by creating three-dimensional mathematical models instead of laboratory tests [35, 36]. Especially in the ANSYS program, FML composites are designed with a practical production method based on the principle of overlapping layers created according to three-dimensional geometric data [36, 37]. In these composite materials, finite element analysis, which is a more effective method than traditional testing methods [37], is used in solving the balance, motion and deformation problems of physical solids [38, 39]. This method is based on continuum mechanics theories [40].

The literature review and analysis show that many theoretical and experimental studies on composite materials have been frequently published in articles by researchers in recent years. In our study, flexural tests of hybrid FML composite materials were performed according to ASTM D7264 standards. For the data obtained, the real-world behaviours of ANSYS program components and subsystems were simulated using the finite element method, and realistic results were obtained.

1.2. Damage Mechanism Caused by Flexural in FML Composites

Four different damage modes occur in FML composite materials. These are matrix mode, delamination mode, fibre mode and penetration. Identifying such modes does not only provide information about flexural [41, 42]. It also allows us to obtain information about the permanent strength of the material. Figure 2 shows the damage types after the flexural test.

Matrix Damages. Matrix damage is the first damage that occurs in the material during dynamic and static loading. Matrix damages; It occurs in the form of matrix fracture or breaking of the interfacial bond of the matrix. In FML composites made of unidirectional fibres, matrix damage occurs in the direction of the fibre [43]. Matrix cracks are less common in thermoplastic materials. Thermoplastic resins change shape more than other resins. Separation between layers is less common in thermoplastic resins [44].

Delamination. Delamination is damage that occurs in composite materials not in the same layer but in different layers, resulting in decreased adhesion between layers. In FML composites, bending stiffness is different due to different fibre orientations in the layers. Delamination occurs due to different bending stiffness. The greater the difference in bending stiffness between layers in FML composites, the greater the delamination.

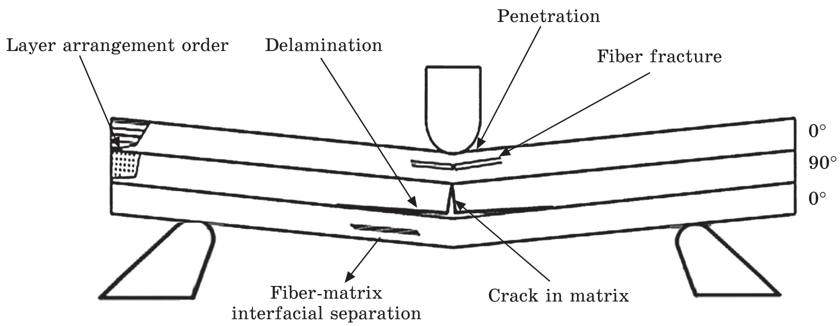

Fig. 2. Damage types occurring in the FML composite material after the flexural test

As a result of the experiments, the worst fibre direction is 0°/90°. Other factors affecting delamination are layer thickness, material properties and stacking order [42–44]. Delamination begins with matrix fracture. Delamination generally occurs in the interface areas. Considering the relationship between matrix fracture and delamination for 0°/90°/0° layers exposed to impact. The fractures, which start in the upper layers, are stopped at the interlayer interface and continue as delamination. The fact that these fractures are stopped at the interlayer interface and continue as delamination is due to the different angle alignments of the fibres. Matrix fractures that lead to delamination are considered critical matrix fractures. It occurs in the form of matrix fracture due to the shear stresses occurring between the layers. Flexural and shear fractures can initiate delamination [18, 43–45].

Fibber Damages. In FML composite materials, fibre damage occurs, matrix cracks and then delamination. The types of fibres used in composite materials are of great importance in the formation of damage. There are features such as energy absorption of composites under static loads, fibre breakage, and high strength. However, if the fibre with high fracture strain is used with a tough resin or a knitted or stitched layer, the composite impact resistance will be improved [15, 17, 19, 40–46].

Fibre–Matrix Interface Separation. Fibre–matrix interface separation is one of the damages seen in low-speed bending tests. Separation at the fibre–matrix interface can reduce or eliminate load transmission from the matrix material to the fibre during flexural. Separation at the fibre–matrix interface generally occurs in un-impacted substrates due to flexural stresses [18, 47].

Penetration. In composite materials, penetration refers to the amount of penetration or penetration of the impacting object on the sample. In composite materials with the same fibre-to-volume ratios but different sizes, the penetration area of the impacting object is generally the same [16, 48, 49].

2. Material Selection and Fabrication Technology

2.1. Material Selection

Since FML composites consist of metal sheets and fibre-reinforced composite material, material selection is very important. However, the properties of these materials significantly affect the mechanical properties of composites. The main load-bearing component in FMLs is fibre-reinforced composite laminates. These laminates largely determine the hardness and strength of FMLs. Metal matrix materials provide different contributions to FMLs such as ductility, impact resistance and energy absorption [2]. Table 1 provides a summary of the basic materials such as matrix, fibre and polymer used in FML composites from relevant literature.

As a result of the literature review, it was seen that aluminium sheets are the most frequently used metallic material in FML composites due to their high impact resistance and superior ductility.

2.2. Fabrication Technology

To use metal matrix elements and fibre-reinforced laminates at full capacity in the production of FML composites, appropriate shaping and curing stages are needed [60, 61]. FMLs are produced using traditional composite techniques. The most common process used to produce FMLs is the autoclave process [62]. Autoclave curing is the most widely used method to produce high-quality laminates in the aerospace industry. Although the autoclave method is generally used in the production of large-size composite materials, it is a production method used to obtain minimum porosity and high product quality [52–63]. It is also another production resin transfer moulding method commonly used in the production of FML composites. The resin infusion process is a dynamic resin flow process that

Table 1. **Literature data on the typical materials used in FML composites**

Ref.	Composite	Matrix material	Fibre Reinforced
[50]	FML	2024-T3 Al	Carbon-reinforced fibre/Epoxy
[51]	FML	2024-T3 Al	Carbon-reinforced fibre/Epoxy
[52]	FML	2024-O Al	Glass fibre reinforced/Polypropylene
[53]	FML	1050 Al	Glass fibre reinforced/Epoxy
[54]	FML	2024-T3 Al	Glass fibre reinforced/Epoxy
[55]	FML	AISI 304L stainless steel	Carbon fibre reinforced/Epoxy Glass fibre reinforced/Epoxy
[56]	FML	7075-T6 Al	Carbon fibre reinforced/Epoxy
[57]	FML	Ti–6Al–4V	Carbon fibre reinforced/Epoxy
[58]	ARALL	6061-T6 Al 7075-T6 Al	Aramid fibre reinforced/Epoxy
[59]	CARALL	5052-H32 Al	Carbon fibre reinforced/Epoxy

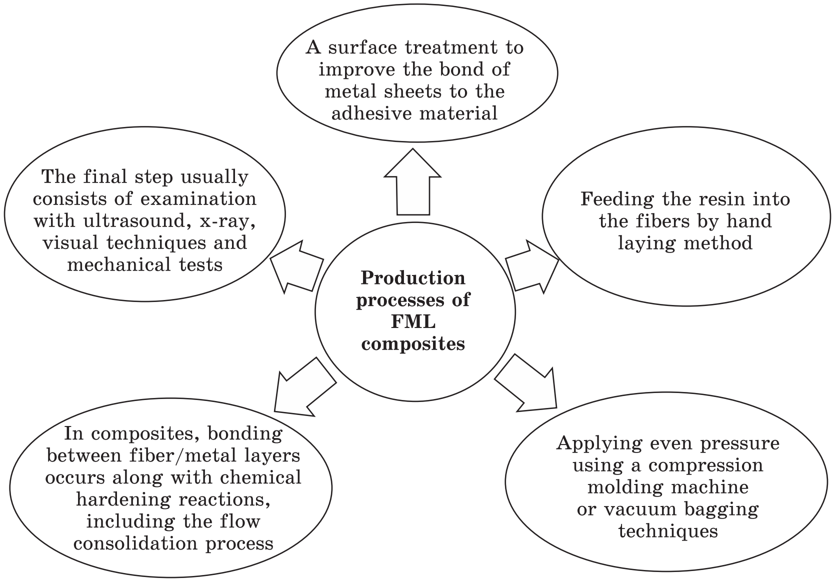

Fig. 3. Production stages of FML composites [59–65]

wets the preform at the bottom of the mild with negative pressure absorbed from the exit of the mild [57–64].

The hot press composite material production method is a fast and practical alternative to other methods. In this method, usually, a ram is mobile and can apply load on a fixed subplate. Heating elements, if present, heat the interior of the atmosphere cabin to the set temperature values. If there is no atmosphere cabin, the resistances in the lower and upper ram heat the composite material pressed between them through heat conduction. In hot pressing systems with an atmosphere cabin, porosity removal by vacuum effect with the help of a vacuum pump positively affects the quality of the final part [64].

The total production of FML composites includes the important steps given in Fig. 3 [59–65].

3. Materials and Methods

3.1. Materials

In the theoretical part of the article, the 3*D* model of FML composites was simulated in the ANSYS program using the finite element method (Fig. 4). The properties of the materials used in the FMLs modelled by the finite element method are compatible with the properties in the real world.

In the experimental part, 1 mm thick 7075-T6 Al sheets were used as matrix material, 0.5 mm thick unidirectional carbon fibre fabric with 300 g/m^2 fibre density and MGS L326 coded epoxy resin were used as fi-

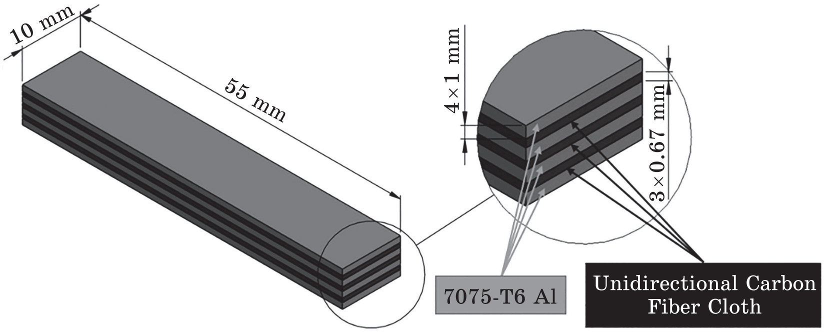

Fig. 4. FML composite sample

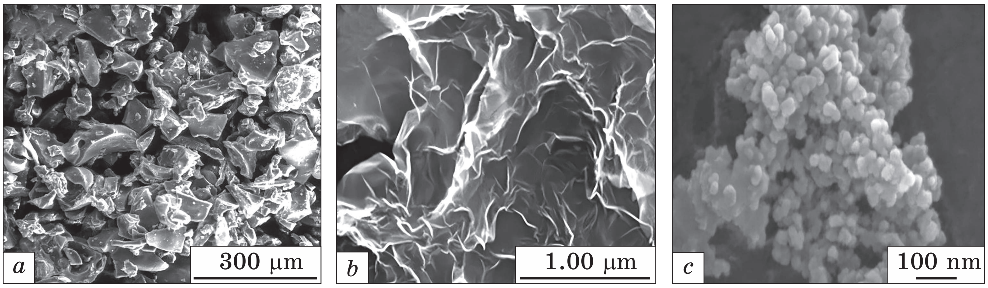

Fig. 5. Scanning electron microscope image of clay (*a*), graphene (*b*), and SiO_2 (*c*) nanoparticles [65]

bres to prepare FML composite samples. At the same time, 15 nm thick clay, 3 nm thick graphene, and 18 nm thick SiO_2 nanoparticles were used as reinforcement phases in FML composite samples. SEM images of nanoparticles are given in Fig. 5 [65].

3.2. Methods

3.2.1. Theoretical Method

We created the mathematical model of the flexural testing of FML composites using the ANSYS Workbench Explicit Dynamics software package according to the ASTM D3039M-17 standard (Fig. 6). This software is based on finite element analysis (FEA). All materials for samples were chosen from the software library.

Composite sample dimensions were taken following the ASTM D7264 standard. Details of the required dimensions are given in Table 2 with the corresponding parameters [66].

Table 2. **Dimensions of the composite sample mm [66]**

Parameter	Value
Length	55
Width	10
Thickness	06

Compound Examples. The designed sample is a composite material consisting of 4 layers of 1 mm thick 7075-T6 Al sheets and

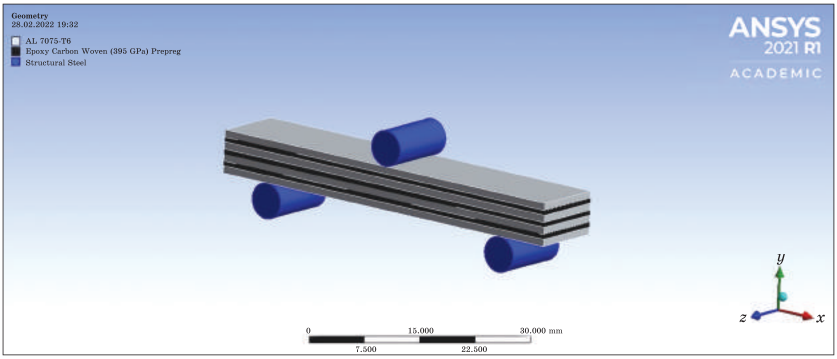

Fig. 6. 3*D* model of flexural test

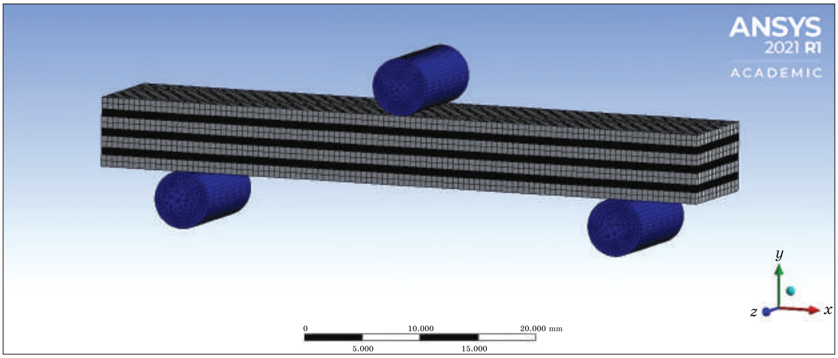

Fig. 7. Meshed flexural test sample

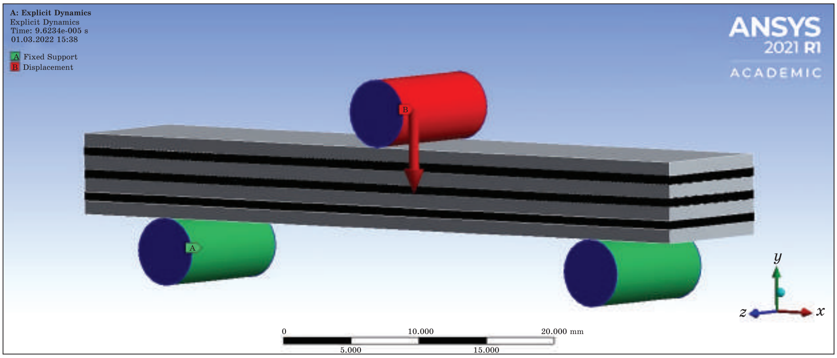

Fig. 8. Boundary conditions for flexural test sample

3 layers of 0.67 mm thick unidirectional carbon fibre fabric. The mechanical properties of 7075-T6 Al sheet and epoxy carbon woven (395 GPa) prepreg are given in Table 3 [66].

Supports. In each test for support, we used 'Structural steel' material, with default parameters from the ANSYS library, which has been given in Table 4 [66].

Table 3. **Properties of 7075-T6 Al sheet and epoxy carbon woven (395 GPa) prepreg [66]**

Material	Density, kg/m³	Young's modulus, GPa	Poisson's ratio	Shear modulus, GPa	Tensile yield strength, GPa
7075-T6 Al sheet	2804	70	0.32	26.7	0.48
Epoxy carbon woven (395 GPa) prepreg	1480	91.8	0.3	3	0.829

Table 4. **Properties of structural steel [66]**

Density, kg/m³	Young's modulus, GPa	Poisson's ratio	Shear modulus, GPa	Tensile yield strength, GPa	Bulk modulus, GPa
7850	200	0.3	70	0.2	166.7

Table 5. **Technical characteristics of the sample [66]**

Volume, m³	Mass, kg	Scale factor value	Bodies	Nodes	Elements	Mesh metric
3.3×10^{-6}	0.00387	1	7	48951	30800	None

Meshing. For the flexural test of FML composites, meshing was performed on the generated sample as shown in Fig. 7. In this test, we have the same meshing properties for specimens, which are shown in Table 5. For the full (specimen and supports together) model of the three-point bending test, there were 66143 nodes (sites) and 45623 elements [66].

Flexural Test. Two extreme support samples were fixed. On the middle support, we applied the displacement equal to 0.17 mm and directed against the Y-axis direction. Boundary conditions for the bending test are shown in Fig. 8.

3.2.2. Experimental Method

In the first stage of the production of FML composites, MGS-L326 epoxy resin and MGS-H265 hardener (100 : 25 ratio) were mixed homogeneously to ensure adhesion between 7075-T6 Al sheets and carbon fibre fabrics. In the second stage, 0.2% graphene, 0.2% clay, and 0.2% SiO_2 nanoparticles were used. These nanoparticles were homogeneously mixed into the epoxy resin using an ultrasonic homogenizer. After cutting the matrix and fibre material into 10×10 cm dimensions, the FML composite samples were stacked in the laboratory environment following the 4/3 stacking rule (Al/CF 0°–CF 0°/Al/CF 0°–CF 0°/Al/CF 0°–CF 0°/Al). The sequence of preparation stages of 7075-T6 Al matrix hybrid FML composite samples is given in Fig. 9 [65].

The prepared samples were pressed in a hot pressing device at a temperature of 120 °C, a pressure of 98 MPa and a protective gas (He) environment for 3 hours. After 3 hours, the FML composite samples were remo-

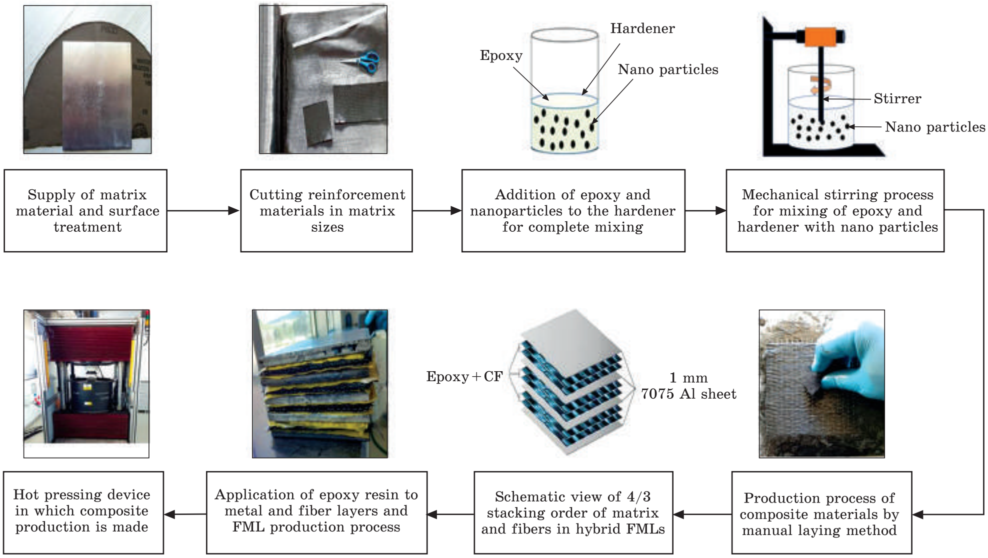

Fig. 9. Production processes of FML composite materials [65]

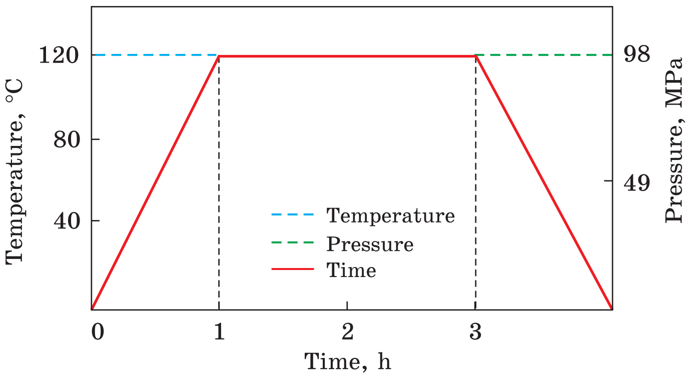

Fig. 10. Curing mode of 7075-T6 Al matrix FML composite samples

ved from the press and cooled at room temperature for 24 hours. The curing mode of 7075-T6 Al matrix FML composite samples is given in Fig. 10.

Flexural Test. To determine the flexural strength properties of FML composite samples, flexural tests were carried out following the ASTM D7264 standard at a flexural speed of 1 mm/min, with a distance of 20 mm between the supports. Flexural tests were carried out in a laboratory environment by removing three flexural samples of 1×10 cm size from each FML composite.

4. Results and Discussions

ANSYS Workbench Explicit Dynamics module of the ANSYS software was used to analyse the flexural test of the composite specimen according to the

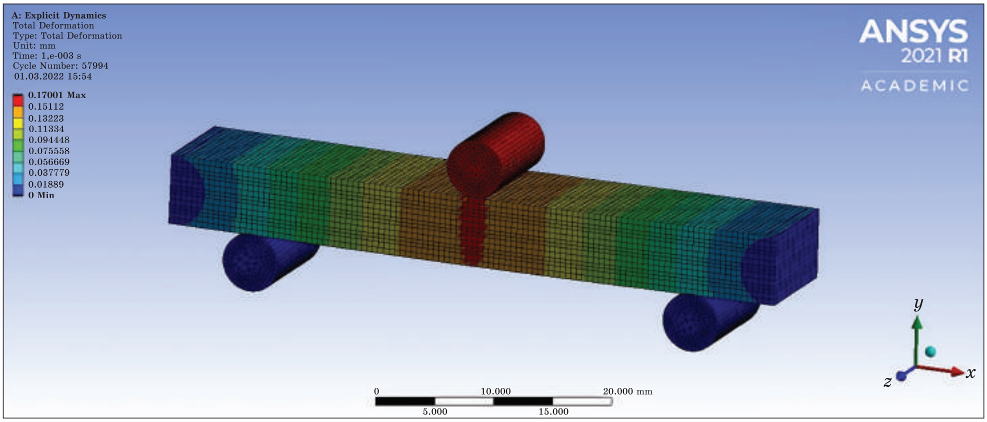

Fig. 11. Total deformation for flexural test sample

ASTM D7264 standard. The same sample was used for test Fig. 4 with the same parameters indicated in Tables 2–5. The process of meshing the specimen is also the same for the test, where the minimum size of the finite element was taken equal to 0.5 mm. The analysis settings for the test are given in Table 6 [66]. Boundary conditions for the flexural test are shown in Fig. 8.

Flexural Test. As stated in the experimental part of the study, flexural tests were performed according to ASTM D7264 to determine the flexural strength properties of 7075-T6 Al-matrix FML composite samples. The experiments were carried out at a flexural speed of 1 mm/min and the distance between supports was 20 mm. As a result of the experiments, it was determined that the stress value during delamination in composite samples was 128.02 MPa and the displacement of the middle support was 0.17 mm. There are many experimental and theoretical studies in the literature to determine the flexural properties of FML composite samples [66, 67]. In Ref. [68], the force–displacement behaviour of two different composite materials was compared experimentally and numerically with the ANSYS finite element method. As a result of these studies, the numerical solution and the experimental solution gave similar results.

For investigation flexural behaviour of our mathematical model Fig. 4, we take the same displacement value during delamination from this experiment, which was equal to 0.17 mm and apply it to our boundary conditions in

Table 6. **Explicit dynamics — analysis settings [66]**

Type	Program Controlled
Step controls	
Number of steps	1
Load step type	Explicit time integration
End time	10^{-3}
Maximum energy error	10^{-1}
Maximum number of cycles	10^{7}

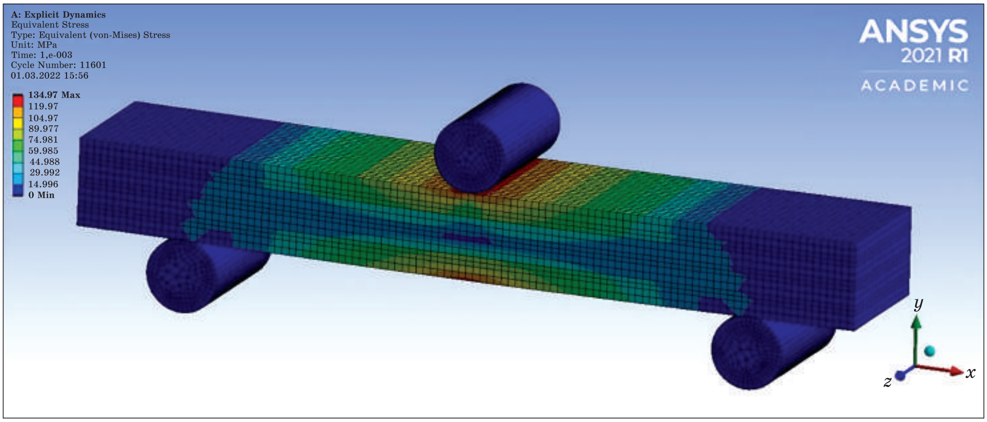

Fig. 12. Equivalent stress for flexural test sample

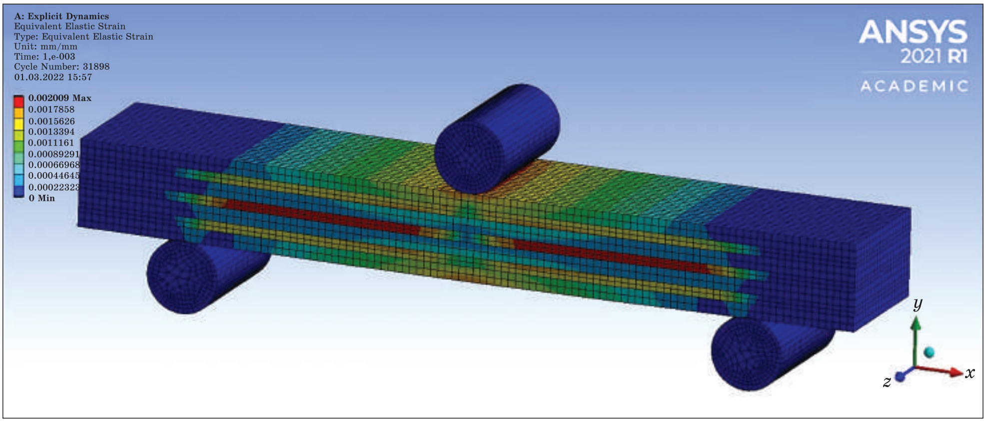

Fig. 13. Equivalent elastic strain for flexural test sample

Fig. 8. After simulation of the bending test, we got results, which are shown in Figs. 11–13. Figure 11 shows a simulation of total deformation where the maximum value occurred on the '7075-T6 Al' and was equal to 0.15619 mm. Figure 12 shows a simulation of equivalent stress where the maximum value occurred on the '7075-T6 Al' and was equal to 134.97 MPa. Figure 13 shows a simulation of equivalent elastic strain where the maximum value occurred on the 'carbon fibre cloth' and was equal to 2.009×10^{-3} mm/mm.

Flexural tests of 7075-T6 Al matrix FML composites with epoxy resin, 0.2% clay, 0.2% graphene, and 0.2% SiO_2 nanoparticle filler were performed at a flexural speed of 1 mm/min according to ASTM D7264 standard. The flexural strength limits of FML composites can be calculated through the flexural tests using the formula

$$\sigma_{\text{flex}} = 3F_{\max} \cdot L/2b \cdot d^2 ,$$

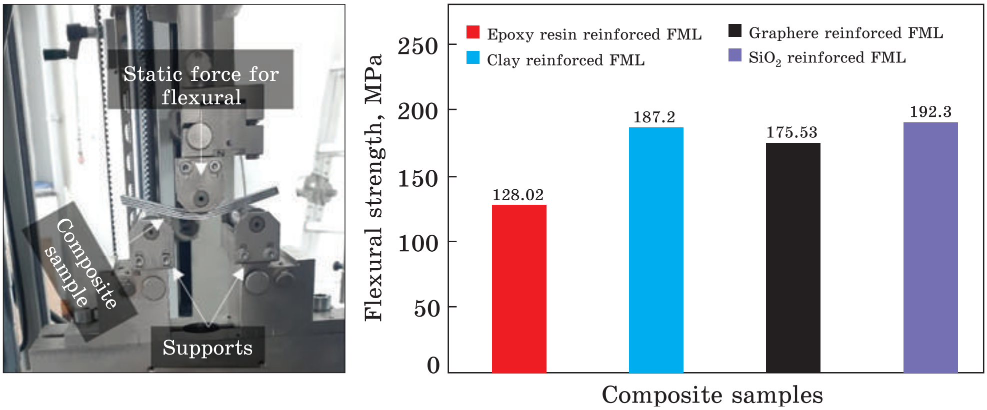

Fig. 14. Flexural test results for FMLs

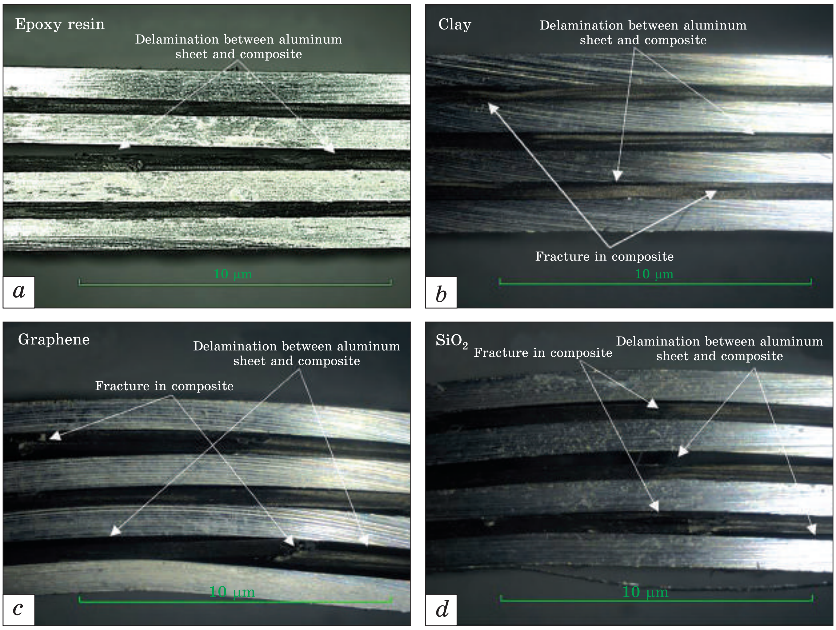

Fig. 15. Microstructure images of FML composite samples after flexural test

where σ_{flex} is the flexural strength value of the composite sample [MPa], F_{max} is the maximum force load damaging the specimen [N], L is the distance between the supports [mm], b is the diameter of the test specimen [mm], and d is a test specimen thickness [mm].

The flexural strength limits of FML composite samples with 7075-T6 Al matrix calculated according to the above-mentioned expression are shown graphically in Fig. 14.

As can be seen from the graph, the flexural strength limit of 7075-T6 Al matrix FML composite samples made with epoxy resin is 128.02 MPa.

In composite samples made with epoxy resin, the flexural strength limit is usually due to the adhesion of the metal matrix and reinforcing fibre layers to each other due to the connections provided by the epoxy resin [69]. When 0.2% clay nanoparticles were used as a filler material in 7075-T6 Al matrix FML composites, it was observed that the flexural strength of the samples was 187.2 MPa and compared to the composites made with epoxy resin, nanoparticles improved the flexural strength of the samples by 46.2%. The unique properties (*i.e.*, small size and high surface area) of 0.2% clay nanoparticles used as filler material in 7075-T6 Al matrix FML composites significantly increase the stiffness and flexural strength of the composite samples by providing inter-plate adhesion. Clay nanoparticles make the composite samples more resistant to deformation under static load [70, 71].

When 0.2% graphene nanoparticles were used as a filler material in 7075-T6 Al matrix FML composites, the flexural strength of the samples was of 175.53 MPa. Compared to the composite samples prepared with epoxy resin, it was determined that the viscosity limit of composites with graphene-nanoparticles' filler increased by 37.11%. Nanoparticles of graphene (a 2*D* carbon allotrope possessing a series of unique properties [72–86]) used as a filler material in FML composite samples create a strong interfacial connection between the matrix and fibres, improve load transfer and prevent crack propagation. This leads to an increase in the tensile and flexural strength limits of the samples [87, 88].

As can be seen from the graph in Fig. 14, when 0.2% SiO_2 nanoparticles were used as a filler material in FML composites with 7075-T6 Al matrix, the flexural strength of the samples was 192.3 MPa. The flexural strength of samples with 0.2% SiO_2 nanoparticle filler increased by 50.2% compared to FML composites made with epoxy resin. Authors of Ref. [89] investigated the effects of different particles such as Al_2O_3, SiO_2, and TiO_2 on the mechanical properties of FML composites. As a result of research, it was observed that SiO_2 particles significantly improved the flexural strength limit of hybrid composite samples.

It was determined during flexural tests that when 0.2% clay, 0.2% graphene and 0.2% SiO_2 nanoparticles were used as filler material in 7075-T6 Al matrix FML composites, the flexural strength of the samples significantly improved. Thus, these nanoparticles prevent the growth of microcracks and delamination in the composite structure [57, 87, 90]. At the same time, nanoparticles strengthen the interfacial connection and ensure better charge transfer between layers [59, 91, 92].

Overall, the addition of nanoparticles to FML composites can offer opportunities for improving strength, stiffness, toughness, fatigue resistance, and interfacial bonding [92, 93]. However, careful selection and optimization of nanoparticle characteristics and processing parameters are necessary to achieve the desired improvements without compromising other important mechanical properties. In this study, the positive effects of the addition of nanoparticles on the flexural properties of FML composites depend on these conditions [92–94].

Interface images of the damaged areas of 7075-T6 Al matrix FML composite samples after bending tests are shown in Fig. 15. Since the adhesion bond between the layers of the FML composite samples prepared with epoxy resin was weaker, delamination between the metal sheets and the composite layers occurs faster (Fig. 15). Since no strong adhesion bond can be formed between sumbata paper polished 7075-T6 Al sheets and epoxy resin, fibre damage is observed to a minimum, and therefore, the amount of deformation in the sheets is small. When nanoparticles are used as filler material in FML composites with 7075-T6 Al matrix, they have a positive effect on inter-plate adhesion properties (Fig. 15)). In the composite samples, the difference between the amount of deformation after the bending tests and the adhesion mechanism from the breaks in the fibres is observed. Since FML composites have low shape-ability, various geometric defects occur in the material during the flexural process [93, 95]. When the experimental studies were examined, tearing, cracking, deformation and separation from the junction area were observed in the materials during the shaping of FML composites [93–96].

5. Conclusions

In this study, a three-dimensional geometric-data-based simulation model of FML composites was created using the finite element method according to the ASTM D3039M standard, and the flexural strength properties were examined experimentally in line with the model.

It was observed that there was a 5% difference between the simulation results made in the ANSYS program and the experimental test results performed to determine the flexural strength properties of FML composite samples.

It was observed as a result of flexural experiments and microstructural analysis that the nanoparticles used in the same proportions in FMLs improved the adhesion bond between the matrix and composite materials and positively affected the flexural strength properties.

REFERENCES

1. E.C. Botelho, R.A. Silva, L.C. Pardini, and M.C. Rezende, *Mater Res.*, **9**, No. 3: 247 (2006).
https://doi.org/10.1590/S1516-14392006000300002
2. L.B. Vogelesang and A. Vlot, *J. Mater. Process Technol.*, **103**, No. 1: 1 (2000).
https://doi.org/10.1016/S0924-0136(00)00411-8
3. S.B. Singh, *SAE Technical Paper*, **26**: 38 (2003).
https://doi.org/10.4271/2003-26-0038
4. S. Nimityongskul, M. Jones, H. Choi, R. Lakes, S. Kou, and X. Li, *Mater. Sci. Eng.*, **527**: 2104 (2010).

5. T.P. Sathishkumar, J. Naveen, and S. Satheeshkumar, *J. Reinf. Plast. Compos.*, **33**, No. 5: 454 (2014).
https://doi.org/10.1177/0731684413516393
6. R. Alderliesten, *Recent Patents Eng.*, **3**, No. 1: 25 (2009).
https://doi.org/10.2174/187221209787259893
7. S. Kumar, R. Singh, and M.S.J. Hasmi, *Adv. Mater. Process. Technol.*, **6**, 1: 13 (2009).
8. J.J.C. Remmer and R. Borst, *Compos. Sci. Technol.,* **61**: 2207 (2001).
https://doi.org/10.1016/S0266-3538(01)00114-2
9. M.R. Abdullah and W.J. Cantwell, *Compos. Sci. Technol.*, **66**, Nos. 11–12: 1682 (2006).
https://doi.org/10.1016/j.compscitech.2005.11.008
10. J. Laliberté, P.V. Straznicky, and C. Poon, *AIAAJ*, **43**, No. 11: 2445 (2005).
https://doi.org/10.2514/1.15159
11. T. Sinmazchelik, E. Avcu, M.O. Bora, and O. Choban, *Mater. Des.*, **32**, No. 7: 3671 (2011).
https://doi.org/10.1016/j.matdes.2011.03.011
12. G.R.Villanueva and W.J. Cantwell. *Compos. Sci. Technol.*, **64**, No. 1: 35 (2004).
https://doi.org/10.1016/S0266-3538(03)00197-0
13. A. Asundi and A.Y.N. Choi, *J. Mater. Process. Technol.*, **63**, Nos. 1–3: 384 (1997).
https://doi.org/10.1016/S0924-0136(96)02652-0
14. R. Alderliesten, C. Rans, and R. Benedictus, *Compos. Sci. Technol.*, **68**, No. 14: 2983 (2008).
https://doi.org/10.1016/j.compscitech.2008.06.017
15. R.C. Alderliesten and R. Benedictus, *J. Aircraft*, **45**, No. 4: 1182 (2008).
https://doi.org/10.2514/1.33946
16. A. Vlot, *Int. J. Impact Eng.*, **18**, No. 3: 291 (1996).
https://doi.org/10.1016/0734-743X(96)89050-6
17. T. Beumler, F. Pellenkoft, A. Tillich, W. Wohlers, and C. Smart, *Airbus Deutschland GmbH*, **1**: 1 (2006).
18. M. Chandrasekar, M.R. Ishak, and M. Jawaid, *J. Reinf. Plast. Compos.*, **36**: 72 (2017).
https://doi.org/10.1177/0731684416668260
19. L.B. Vogelesang and A. Vlot, *J. Mater. Process. Technol.*, **103**, No. 1: 1 (2000).
https://doi.org/10.1016/S0924-0136(00)00411-8
20. J. Fan, Z.W. Guan, and W.J. Cantwell, *Compos. Struct.*, **93**, No. 9: 2430 (2011).
https://doi.org/10.1016/j.compstruct.2011.04.008
21. R. Eslami-Farsani, H. Aghamohammadi, and H. Jalali, *J. Industrial Textiles*, **51**, No. 5: 7374 (2022).
https://doi.org/10.1177/1528083720947106
22. A. Afrouzian, A.H. Movahhedi, and G. Liaghat, *J. Reinf. Plast. Compos.*, **36**, No. 12: 900 (2017).
https://doi.org/10.1177/0731684417694753
23. K.T. Lau, C. Gu, and D. Hui, *Compos. Part B: Eng.*, **37**, No. 6: 425 (2006).
https://doi.org/10.1016/j.compositesb.2006.02.020
24. N. Zareei, A. Geranmayeh, and R. Eslami-Farsani, *Polym. Test*, **75**: 205 (2019).
https://doi.org/10.1016/j.polymertesting.2019.02.002
25. F. Bahari, S.R. Eslami, and S.A. Chirani, *J. Sandwich Struct. Mater.*, **22**, No. 6: 1931 (2020).
https://doi.org/10.1177/1099636218792693

26. S.N. Abbandanak, M.A. Azghan, and H. Siadati, *J. Industrial Textiles*, **51**, No. 2: 2576 (2022).
https://doi.org/10.1177/1528083720932222
27. M. Megahed, M.A. Abd El-baky, A.M. Alsaeedy, and A.E. Alshorbagy, *Compos. Part B: Eng.*, **176**, No. 1: 107277 (2019).
https://doi.org/10.1016/j.compositesb.2019.107277
28. H. Aghamohammadi, S.N.H. Abbandanak, R. Eslami-Farsani, and S.H. Siadati, *Int. J. Adhes. Adhes.*, **84**: 184 (2018).
https://doi.org/10.1016/j.ijadhadh.2018.03.005
29. M.A. Azghan and R.E. Farsani, *Mater. Res. Express*, **5**, No. 2: 025302 (2018).
https://doi.org/10.1088/2053-1591/aaa92c
30. M.S. Maryan, H. Ebrahimnezhad-Khaljiri, and R. Eslami-Farsani, *Int. J. Fatigue*, **154**: 106560 (2022).
https://doi.org/10.1016/j.ijfatigue.2021.106560
31. M.E. Mehr, H. Aghamohammadi, S.H. Abbandanak, G.R. Aghamirzadeh, R. Eslami-Farsani, and S. Siadati, *Int. J. Adhes. Adhes.*, **92**: 133 (2019).
https://doi.org/10.1016/j.ijadhadh.2019.04.015
32. G.S. Dhaliwal and G.M. Newaz, *Compos. Struct.*, **160**: 1212 (2017).
https://doi.org/10.1016/j.compstruct.2016.11.015
33. E.J. Barbero and M. Shahbazi, *Mater. Today: Proc.*, **176**: 768 (2017).
https://doi.org/10.1016/j.compstruct.2017.05.074
34. L. Li, L. Sun, T. Wang, N. Kang, and W. Cao, *Aerosp. Sci. Technol.*, **84**: 995 (2019).
https://doi.org/10.1016/j.ast.2018.11.038
35. C. Chen, H. Fang, L. Zhu, J. Han, X. Li, and Z. Qian, *Compos. Struct.*, **306**: 116573 (2023).
https://doi.org/10.1016/j.compstruct.2022.116573
36. P.Y. Chang, P.C. Yeh, and J.M. Yang, *Mater. Sci. Eng. A*, **496**, Nos. 1–2: 273 (2008).
https://doi.org/10.1016/j.msea.2008.07.041
37. J.H. Jin and R.C. Batra, *Mater. Sci. Eng. A*, **216**, Nos. 1–2: 117 (1996).
https://doi.org/10.1016/0921-5093(96)10396-8
38. T. Tomasetti, *AIAA Journal*, **53**, No. 8: 2228 (2015).
https://doi.org/10.2514/1.J053600
39. M.J. Jweeg, A.S. Hammood, and M. Al-Waily, *J. Sci. Technol.*, **2**, No. 8: 697 (2015).
40. P. Soltani, M, Keikhosravy, R.H. Oskouei, and C. Soutis, *Appl. Compos. Mater.*, **18**, No. 4: 271 (2011).
https://doi.org/10.1007/s10443-010-9155-x
41. A. Vlot, R.C. Alderliesten, P.A. Hooijmeijer, J.L.C.G. de Kanter, J. Sinke, and M.S. Ypma, *Int. J. Mater. Prod. Technol.*, **17**, Nos. 1–2: 79 (2002).
https://doi.org/10.1504/IJMPT.2002.001301
42. A. Vlot, *Composite Eng.*, **3**, No. 10: 911 (1993).
https://doi.org/10.1016/0961-9526(93)90001-Z
43. M. Sadighi, R.C. Alderliesten, and R. Benedictus, *Int. J. Impact Eng.*, **49**: 77 (2012).
https://doi.org/10.1016/j.ijimpeng.2012.05.006
44. W.J. Cantwell and J. Morton, *Composites*, **22**, No. 5: 347 (1991).
https://doi.org/10.1016/0010-4361(91)90549-V
45. R. Costa, R. Sales-Contini, F. Silva, N. Sebbe, and A. Jesus, *Metals*, **13**, No. 4: 638 (2023).
https://doi.org/10.3390/met13040638

46. P. Compston, W.J. Cantwell, C. Jones, and N. Jones, *J. Mater. Sci.*, **20**, No. 7: 597 (2001).
https://doi.org//10.1023/A:1010904930497
47. J.F. Laliberte, C. Poon, P.V. Strazincky, and A. Fahr, *Polym. Composites*, **21**, No. 4: 558 (2000).
https://doi.org/10.1002/pc.10211
48. B. Wang and T. Siegmund, *Int. J. Fract.*, **132**, No. 2: 575 (2005).
https://doi.org/10.1007/s10704-005-0627-1
49. L. Ye, A. Afaghi-Khatibi, G. Lawcock, and Y.W. Mai, *Compos. Part A*, **29**, No. 12: 1525 (1998).
https://doi.org/10.1016/j.matdes.2011.03.011
50. L. Yao, C.Z. Wang, W.T. He, S.J. Lu, and D. Xie, *Thin-Walled Struct.*, **145**: 106399 (2019).
https://doi.org/10.1016/j.tws.2019.106399
51. L. Yao, G.Y. Sun, W.T. He, X.J. Meng, and D. Xie, *Compos. Struct.*, **226**: 111218 (2019).
https://doi.org/10.1016/j.compstruct.2019.111218
52. T.P. Vo, Z.W. Guan, W.J. Cantwell, and G.K. Schleyer, *Compos. Struct.*, **94**, No. 3: 954 (2012).
https://doi.org/10.1016/j.compstruct.2011.10.027
53. M.H. Kashani, M. Sadighi, A. Lalehpour, and R.C. Alderliesten, *J. Compos. Mater.*, **49**, No. 6: 635 (2015).
https://doi.org/10.1177/0021998314521476
54. A.P. Sharma, S.H. Khan, R. Kitey, and V. Parameswaran, *Polym. Test.*, **65**: 311 (2018).
https://doi.org/10.1016/j.polymertesting.2017.12.001
55. T. Parnanen, M. Kanerva, E. Sarlin, and O.J.C.S. Saarela, *Compos. Struct.*, **119**: 775 (2015).
https://doi.org/10.1016/j.compstruct.2014.09.056
56. T. Pärnänen, A. Vänttinen, M. Kanerva, J. Jokinen, and O. Saarela, *Appl. Compos. Mater.*, **23**: 1151 (2016).
https://doi.org/10.1007/s10443-016-9505-4
57. X. Li, X. Zhang, Y. Guo, V.P.W. Shim, J. Yang, and G.B. Chai, *Int. J. Impact Eng.*, **114**: 32 (2018).
https://doi.org/10.1016/j.ijimpeng.2017.12.011
58. C. Kaboglu, I. Mohagheghian, and J.P. Dear, *J. Mater. Sci.*, **53**: 4209 (2018).
https://doi.org/10.1007/s10853-017-1871-2
59. G.S. Dhaliwal and G.M. Newaz, *Behav. Mater.*, **2**: 399 (2016).
https://doi.org/10.1007/s40870-016-0075-1
60. H.H. Kim, M.S. Lee, and C.G. Kang, *Mater. Manuf. Process.*, **28**, No. 8: 892 (2013).
61. M.E. Kazemi, L. Shanmugam, L. Yang, and J. Yang, *Compos. Part A*, **128**: 54 (2020).
62. A. Salve, R. Kulkarni, and A. Mache, *Int. J. Eng. Technol. Sci.*, **6**, No. 1: 71 (2016).
https://doi.org/10.15282/ijets.6.2016.10.2.1060
63. H. Ahmadi, G.H. Liaghat, H. Sabouri, and E. Bidkhouri, *J. Compos. Mater.*, **47**: 1605 (2013).
https://doi.org/10.1177/0021998312449883
64. V.G. Reyes and W.J. Cantwell, *J. Mater. Process. Technol.*, **186**, Nos. 1–3: 284 (2000).
https://doi.org/10.1016/j.jmatprotec.2006.12.050

65. N. Gurbanov, *Adv. Phys. Res.*, **5**, No. 3 146 (2023).
66. M. Babanli, Y. Turen, N. Gurbanov, R. Mehtiyev, M.Y. Askin, and M. Ismayilov, *J. Appl. Comp. Mech.*, **9**, No. 4: 987 (2023).
https://doi.org/10.22055/JACM.2023.42798.3978
67. M. Smolnicki, Sz. Duda, P. Stabla, and T. Osiecki, *Compos. Struct.*, **313**: 116943 (2023).
68. Y.P. Ravitej, V. Swaroop, S. Ramesh, and H. Adarsha, *IOP Conf. Series: Mater. Sci. Eng.*, **376**: 012040 (2018).
69. G.R. Rajkumar, M. Krishna, H.N. Narasimhamurthy, Y.C. Keshavamurthy, and J.R. Nataraj, *Proc. Mater. Sci.*, **5**: 60 (2014).
70. M.W. Ho, C.K. Lam, and K.T. Lau, *Compos. Struct.*, **75**, Nos. 1–4: 415 (2006).
https://doi.org/10.1016/j.compstruct.2006.04.051
71. M.H. Pol, G.H. Liaghat, and E.M. Yeganeh, *Modares Mech. Eng.*, **14**: 76 (2015).
72. S.P. Repetsky, I.G. Vyshyvana, S.P. Kruchinin, V.B. Molodkin, and V.V. Lizunov, Influence of the adsorbed atoms of potassium on an energy spectrum of graphene, *Metallofiz. Noveishie Tekhnol.*, **39**, No. 8: 1017 (2017).
https://doi.org/10.15407/mfint.39.08.1017
73. O.S. Skakunova, S.I. Olikhovskii, T.M. Radchenko, S.V. Lizunova, T.P. Vladimirova, and V.V. Lizunov, X-ray dynamical diffraction by quasi-monolayer graphene, *Sci. Rep.*, **13**: 15950 (2023).
https://doi.org/10.1038/s41598-023-43269-6
74. A.G. Solomenko, R.M. Balabai, T.M. Radchenko, V.A. Tatarenko, Functionalization of quasi-two-dimensional materials: chemical and strain-induced modifications, *Prog. Phys. Met.*, **23**, No. 2: 147 (2022).
https://doi.org/10.15407/ufm.23.02.147
75. T.M. Radchenko, I.Yu. Sahalianov, V.A. Tatarenko, Yu.I. Prylutskyy, P. Szroeder, M. Kempiński, and W. Kempiński, Strain- and adsorption-dependent electronic states and transport or localization in graphene, *Springer Proceedings in Physics: Nanooptics, Nanophotonics, Nanostructures, and Their Applications* (Eds. O. Fesenko and L. Yatsenko) (Cham, Switzerland: Springer: 2018), vol. **210**, ch. 3, p. 25.
https://doi.org/10.1007/978-3-319-91083-3_3
76. T.M. Radchenko, V.A. Tatarenko, and G. Cuniberti, Effects of external mechanical or magnetic fields and defects on electronic and transport properties of graphene, *Mater. Today: Proc.*, **35**, pt. 4: 523 (2021).
https://doi.org/10.1016/j.matpr.2019.10.014
77. I.Yu. Sagalianov, T.M. Radchenko, V.A. Tatarenko, and G. Cuniberti, Sensitivity to strains and defects for manipulating the conductivity of graphene, *EPL*, **132**: 48002 (2020).
https://doi.org/10.1209/0295-5075/132/48002
78. P. Szroeder, I. Sahalianov, T. Radchenko, V. Tatarenko, and Yu. Prylutskyy, The strain- and impurity-dependent electron states and catalytic activity of graphene in a static magnetic field, *Optical Mater.*, **96**: 109284 (2019).
https://doi.org/10.1016/j.optmat.2019.109284
79. P. Szroeder, I.Yu. Sagalianov, T.M. Radchenko, V.A. Tatarenko, Yu.I. Prylutskyy, and W. Strupiński, Effect of uniaxial stress on the electrochemical properties of graphene with point defects, *Appl. Surf. Sci.*, **442**: 185 (2018).
https://doi.org/10.1016/j.apsusc.2018.02.150
80. I.Yu. Sahalianov, T.M. Radchenko, V.A. Tatarenko, and Yu.I. Prylutskyy, Magnetic field-, strain-, and disorder-induced responses in an energy spectrum of gra-

phene, *Ann. Phys.*, **398**: 80 (2018).
https://doi.org/10.1016/j.aop.2018.09.004
81. T.M. Radchenko and V.A. Tatarenko, A statistical-thermodynamic analysis of stably ordered substitutional structures in graphene, *Physica E*, **42**, No. 8: 2047 (2010).
https://doi.org/10.1016/j.physe.2010.03.024
82. D.M.A. Mackenzie, M. Galbiati, X.D. de Cerio, I.Y. Sahalianov, T.M. Radchenko, J. Sun, D. Peca, L. Gammelgaard, B.S. Jessen, J.D. Thomsen, P. Bøggild, A. Garcia-Lekue, L. Camilli, and J.M. Caridad, Unraveling the electronic properties of graphene with substitutional oxygen, *2D Materials*, **8**, No. 4: 045035 (2021).
https://doi.org/10.1088/2053-1583/ac28ab
83. T.M. Radchenko, I.Yu. Sahalianov, V.A. Tatarenko, Yu.I. Prylutskyy, P. Szroeder, M. Kempiński, and W. Kempiński, The impact of uniaxial strain and defect pattern on magnetoelectronic and transport properties of graphene, *Handbook of Graphene: Growth, Synthesis, and Functionalization* (Eds. E. Celasco and A. Chaika) (Beverly, MA: Scrivener Publishing LLC: 2019), vol. **1**, ch. 14, p. 451.
https://doi.org/10.1002/9781119468455.ch14
84. T.M. Radchenko, V.A. Tatarenko, V.V. Lizunov, V.B. Molodkin, I.E. Golentus, I.Yu. Sahalianov, and Yu.I. Prylutskyy, Defect-pattern-induced fingerprints in the electron density of states of strained graphene layers: diffraction and simulation methods, *Phys. Status Solidi B*, **256**, No. 5: 1800406 (2019).
https://doi.org/10.1002/pssb.201800406
85. T.M. Radchenko, V.A. Tatarenko, I.Yu. Sagalianov, and Yu.I. Prylutskyy, Configurations of structural defects in graphene and their effects on its transport properties, *Graphene: Mechanical Properties, Potential Applications and Electrochemical Performance* (Ed. B.T. Edwards) (New York: Nova Science Publishers: 2014), ch. 7, p. 219.
86. I.Yu. Sagalyanov, Yu.I. Prylutskyy, T.M. Radchenko, and V.A. Tatarenko, Graphene systems: methods of fabrication and treatment, structure formation, and functional properties, *Usp. Fiz. Met.*, **11**, No. 1: 95 (2010).
https://doi.org/10.15407/ufm.11.01.095
87. J.P.S. Ahmed and O. Meenakshisundaram, *Eng. Res. Express*, **4**: 025021 (2022).
https://doi.org/10.1088/2631-8695/ac6e30
88. S. Wang, M. Cao, H. Xue, Sh. Araby, and Q. Meng, *Thin-Walled Structures,* **174**: 109092 (2022).
https://doi.org/10.1016/j.tws.2022.109092
89. Y. Arao, S. Yumitori, and H. Suzuki, *Compos. Part A: Appl. Sci. Manuf.*, **55**: 19 (2013).
https://doi.org/10.1016/j.compositesa.2013.08.002
90. A.R. Sadygova, I.I. Abbasov, E.S. Safiev, P.B. Asilbeyli, and V.A. Alekperov, *Nanosistemi, Nanomateriali, Nanotehnologii*, **17**, No. 1: 155 (2019).
https://doi.org/10.15407/nnn.17.01.155
91. A. Royani, C. Verma, M. Hanafi, V.S. Aigbodion, and A. Manaf, *Prog. Phys. Met.*, **24**, No. 1: 197 (2023).
https://doi.org/10.15407/ufm.24.01.197
92. R.C. Ganesh and N. Lalit, *Mater. Today: Proc.*, **27**, No. 1: 272 (2020).
https://doi.org/10.1016/j.matpr.2019.08.240
93. H. Xiao, M.T.H. Sultan, and D. Hui, *Rev. Adv. Mater. Sci.*, **62**: 20220328 (2023).
https://doi.org/10.1515/rams-2022-0328
94. H.E. Etri, M.E. Korkmaz, M.K. Gupta, M. Gunay, and J. Xu, *Int. J. Adv. Manuf. Technol.*, **123**: 2965 (2022).
https://doi.org/10.1007/s00170-022-10277-1

95. P. Zuo, D.V. Srinivasan, and P.V. Anastasios, *Compos. Struct.*, **274**: 114358 (2021). https://doi.org/10.1016/j.compstruct.2021.114358
96. W. He, L. Wang, H. Liu, C. Wang, and G. Sun, *Thin-Walled Struct.*, **167**: 108026 (2021).
https://doi.org/10.1016/j.tws.2021.108026

Received 08.04.2024
Final version 03.05.2024

Н.А. Гурбанов
Азербайджанський державний нафтопромисловий університет,
Азадліг, 20,
1010 Баку, Азербайджан

ЕКСПЕРИМЕНТАЛЬНИЙ МЕТОД І МЕТОД СКІНЧЕННИХ ЕЛЕМЕНТІВ У ВИЗНАЧЕННІ ВЛАСТИВОСТЕЙ ЗА ВИГИНУ ВОЛОКНИСТИХ МЕТАЛЕВИХ ЛАМІНАТНИХ КОМПОЗИТІВ

З метою ліпшої інтерпретації процесів пошкодження, що відбуваються у зразках композитів із волокнистих металевих ламінатів (ВМЛ) виконано двоетапне дослідження. На першому етапі було створено тривимірну модель композитів ВМЛ на основі геометричних даних за допомогою методу скінченних елементів і використано його для прогнозування властивостей міцності на вигин відповідно до стандарту ASTM D3039M. На другому етапі зразки 7075-T6 Al матриці ВМЛ із додаванням наночастинок 0,0% епоксидної смоли, 0,2% графену, 0,2% SiO_2 і 0,2% глини було виготовлено в лабораторних умовах відповідно до чисельної моделі і досліджено їхні властивості міцності на вигин. У результаті експериментів виявлено, що додавання 0,2% наночастинок SiO_2 поліпшує властивості міцності на вигин зразків ВМЛ матриці 7075-T6 Al на 50,2% порівняно з такими властивостями композитів, виготовлених з епоксидною смолою. Це значення є найвищим показником міцності на вигин серед груп зразків з однаковим співвідношенням. Також виявлено різницю у 5% між результатами випробувань на вигин композитних зразків ВМЛ, виготовлених згідно зі стандартом ASTM D3039M, і результатами моделювання, виконаного в рамках програми ANSYS.

Ключові слова: композит із волокнистих металевих ламінатів, міцність на вигин, наночастинки, метод скінченних елементів.